Proceedings of ASME Turbo Expo 2011
GT2011
June 6-10, 2011, Vancouver, British Columbia, Canada

GT2011-45752

EVALUATION OF A WIRE-MESH DUCT BURNER PREMIXER USING LSI TECHNIQUES

Omar B. Ramadan
CanmetENERGY Centre, NRC
Nepean, Ontario, Canada.
oramadan@nrcan.gc.ca

Patrick M. Hughes
CanmetENERGY Centre, NRC
Nepean, Ontario, Canada.
phughes@nrcan.gc.ca

J. E. Donald Gauthier
Power Systems Manufacturing (PSM), Jupiter, Florida, USA
donald.gauthier@psm.com

1 ABSTRACT

The mixing of fuel and oxidizer is critical for the reduction of NOx emissions from premixed combustion burners. The mixing process in a pre-mixer of a natural gas-fired conical wire-mesh duct burner (DB) was studied experimentally using the laser sheet illumination (LSI) technique. A quasi-quantitative technique was used to rank the relative mixing performance of the different geometrical and flow combinations tested (mixer geometry, fuel injection angle and fuel air momentum ratio).The present paper presents some of the results used in the design and analysis of the burner. This burner was integrated and tested with a micro-turbine cogeneration system (MT70 kW Ingersoll Rand (IR) CHP unit). The DB provides supplementary firing in the exhaust gas stream of the micro-turbine to increase and control the thermal output of the micro-cogeneration system. The combination provided near perfect premixing and low emissions. The DB successfully raised the micro-turbine exhaust gas temperature from about 227ºC to as high as 700ºC with NOx and CO emissions of less than 5 ppm and 10 ppmv (corrected to 15 percent O_2) respectively. The DB also displayed stable, low emissions operation throughout the surface firing rate range of 148 kW to 328 kW (1574 kW/m^2 to 3489 kw/m^2). The results show that LSI technique can provide invaluable information about the overall flow field structure. Many important observations are discussed such as mixing, fuel spread, and fuel jet penetration. Samples of the LSI images and 3D plots for selected cases are presented. The two best geometrical combinations ranked during the LSI test were used in the actual combustion test of the DB. Some of the combustion results which prove the effectiveness of the LSI technique are presented.

Keywords: LSI, unmixedness, Low NO_x mesh burner, microturbine

2 INTRODUCTION

This study forms part of an investigation into the design and evaluation a low NOx, natural gas-fired, mesh DB for a micro-cogeneration unit. As an overview, the main work relates to the integration of a micro-turbine power plant and a supplementary firing burner in the micro-turbine exhaust gas. This secondary fuel burner is used to improve the quantity and the quality of the heat content of the exhaust gas to a point where it can be used as a heat source for a number of purposes, such as for an absorption chiller, with the lowest increase in NOx formation. Fig.1 presents the general concept of the supplementary-fired micro-CHP system as used in the main work. Previous papers reported some of the experimental results from this project. Ref. [1] provides experimental results representing the effects of some parameters such as pressure drop, excess air and firing rate on the stable burning zones and emissions (NOx and CO) of the DB. In Ref. [2] the design procedure of the wire-mesh DB was presented. As a continuation of the above, the present paper focuses on the mixing process inside the premixer of the DB. This process was examined by performing qualitative flow visualization tests.

In general flow visualization has played a very important role in the improvement of understanding different fluid flow problems [3 and 4]. Flow visualization is a technique that can give qualitative information about a flow field. However, using high speed digital cameras, lasers and advanced image analysis, it is possible to derive quantitative information about the flow field. A large variety of flow visualization techniques are available for different flow conditions. For more details on the different techniques used and their principles, refer to Refs. [3 to 8]. The Mie scattering technique using a laser sheet is one of the flow visualization techniques used by different researchers [e.g., 9 to 14]. The planar Mie scattering technique is a diagnostic approach that produces images of the flow field and has widely been used for flow visualization in gas phase flows due to its simplicity [4]. The basic idea of the laser sheet visualization technique is to illuminate a seeded flow by means of a sheet of laser light and to record the scattered light. The planar Mie scattering technique was adopted in this study to identify the design and operating parameters that will provide rapid and enhanced mixing between the oxidant (microturbine exhaust gases) and the fuel inside the duct burner premixer.

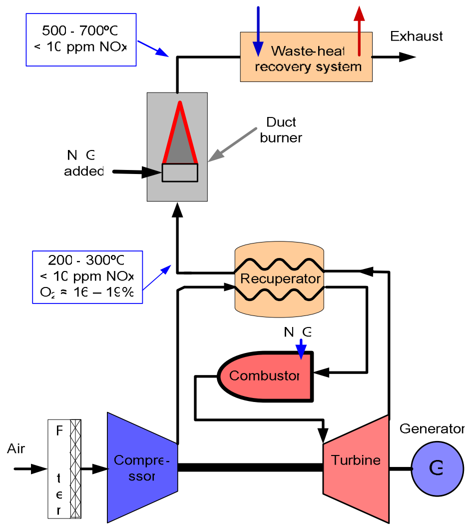

Fig.1: General concept of a micro-CHP system with an integrated duct burner

The LSI or LSV (V for visualization) technique is a non-intrusive optical diagnostic procedure which is relatively inexpensive and can quickly demonstrate how flow fields interact. In this study, using this technique, a laser sheet illuminates the plane of interest (a two-dimensional cross-section) inside the premixer so that the air and "fuel" jet mixing can be easily recorded as images. The images provided by this technique show the occurrence of regular, periodic structures in the flow field under observation.

3 EXPERIMENTAL SETUP AND ANALYSIS

The LSI technique used here consists of two main components, the experimental acquisition of images (test rig, laser and optics) and the computer image processing and analysis. This section includes a brief description of the various components of the LSI system used in the present study.

3.1 PREMIXER TEST RIG

The premixer test facility was designed and set up to study the mixing process. The test rig is made of Plexiglas to permit optical access. The premixer was tested at full scale in this fully transparent test rig. A relatively long premixer tube was used to minimize the effect of flow turning at the premixer exit. During the design of the LSI experiment, to achieve similarity between the real flow field and the flow used in the LSI tests, the two main parameters to be considered are the geometry and Reynolds number. Geometrical similarity was achieved using the full-scale premixer (same dimensions). The Reynolds number (Re) for the real flow situation tests is sufficiently high (Re > 50000) and as such the flow is dominated by turbulent mixing. For this reason the momentum ratio (defined in Eq.1) was the parameter matched between the real model (duct burner) and the physical or cold flow LSI model.

$$MMR = \frac{\dot{m}_{fuel} V_{fuel}}{\dot{m}_{flow} V_{flow}} \quad (1)$$

where MMR, $\dot{m}_{fuel}$, $\dot{m}_{flow}$, V_{fuel} and V_{flow} respectively are the momentum ratio, fuel stream mass flow rate, mainstream mass flow rate, fuel exit velocity and the mainstream inlet velocity.

Figure 2 shows the Plexiglas premixer (test section) and the relevant dimensions. The premixer has a centrally positioned fuel tube, coaxial with the swirling flow where the swirling flow is introduced through a static mixer of different designs. The swirling flow mixers are known as high effectiveness mixing devices, which shortens the mixing length, especially when limited space is available, as in the case of the duct burner under investigation.

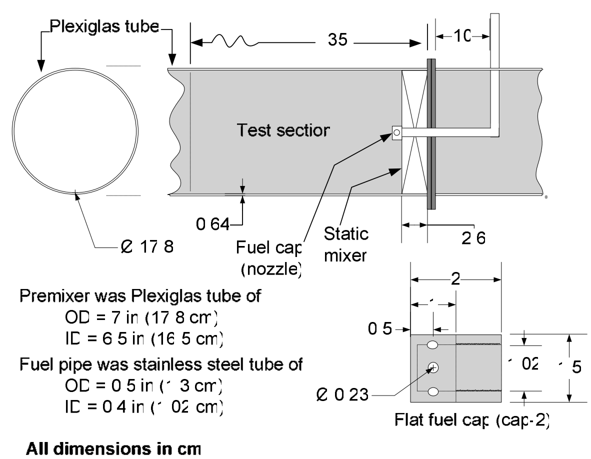

Fig.2: Schematic of the Plexiglas test section and its dimensions.

Two different fuel injection methods were investigated. (1) transverse injection through eight holes, drilled at 90 degrees to the co-flowing air stream (referred to as flat caps) and (2) transverse injection through the same number of holes drilled at 45 degrees (referred to as round caps). For more details regarding the DB premixer and its components refer to Ref. [2]. During the tests, the premixer model was installed in the Plexiglas tank at the adapter and air was supplied to the "fuel" and air inlet of the premixer. In this case, air simulated both the fuel and micro-turbine exhaust gases flowing through an actual test rig. The air supply system consisted of a forced-draft fan, which supplied the air for the test rig. The flows were regulated and monitored by a CPU-based control station. The air supply system could supply the two inlets, gas and air, ranging from 0 to 55 CFM for the gas and 0 to 800 CFM for the air. During the tests the "fuel" flow was seeded uniformly with alumina particles (Al_2O_3), to distinguish it from the main air flow and to follow the mixing. The Al_2O_3 particles mean diameter was 6 μm. A small fluid bed feeder fluidized with dry compressed air with controls for the pressure and flow rate was used to feed the alumina particles into the test section.

3.2 LASER AND OPTICS SETUP

The laser sheet used to illuminate the plane of interest inside the burner premixer for this work was produced by a 2 W Argon Ion Continuous Wave Laser operating at a single-line at 514.5 nm with a beam diameter of 1.3 mm. The laser was formed into a vertical sheet by a 6.35 mm focal length cylindrical lens. The sheet thickness was approximately 2 mm throughout the test section measurement area. The laser light sheet has a Gaussian intensity profile [15].

3.3 IMAGING EQUIPMENT

The Imaging equipment used in this investigation is divided into two parts: (1) the camera and (2) the data acquisition system. The camera used to record the images during this phase of the thesis was a water cooled Princeton Instruments (PI) **I**ntensified **C**harge **C**oupled **D**evice (ICCD) camera with a 576 × 384 full frame CCD pixel array. Nitrogen was used to continuously flush of the detector to avoid condensation on the CCD. The data acquisition system connected to the detector consisted of a controller and a pulse generator. The controller (PI, model ST-130) was used to regulate the internal temperature of the camera, to receive the data from the camera and transmit it to the computer, where it could be viewed as an image in "real time" using the WinView software.

3.4 IMAGE PROCESSING

To ensure accurate visual representation of the flow field as a digital image, a correction procedure was applied to each image. The images were corrected for the intensity variation across the laser sheet, background (noise) and any variation in the response of the ICCD camera pixels [7]. After the acquired images were corrected for the laser non-uniformity, the images were corrected for the variation in response of the CCD camera, pixel by pixel, using the following formula [16]:

$$CI = \frac{(ADI)-(BGI)}{(FFI)}(AI_{FFI}) \qquad (2)$$

where CI is the corrected image (frame), ADI is the original acquired data image corrected for light non-uniformity, BGI is the background image, FFI is the flat field image (as a normal data file) and AI_{FFI} is the average light intensity of the flat field image corrected from the CCD fixed pattern signals (dark charge). A dark charge frame (DCI) should be subtracted from all types of collected images, such as the background $(BGI-DCI)$ and the flat field images $(FFI-DCI)$.

The dark charge frame is the fixed pattern signal that occurs with no light incident on the camera. It is captured with no illumination into the camera or by a completely blocked detector (when the lens cap is on). This frame accounts for pixels which have an offset from zero. The background frame is due to reflections of the laser from walls and windows or particles not of interest and external light sources. The background image was taken with the laser running and without the scattering particles. This background image is also affected by the dark charge of the detector. Therefore, the dark charge image had to be subtracted from the background image. The flat-field or the white-field frame image is due to a non-uniform pixel response. This was done by illuminating a flat, uniform white surface (card) and capturing an image of the surface with the camera. This image is also corrected for the dark charge. In the present work, to achieve a uniform light distribution, a flat-field box was used, see Fig.3.

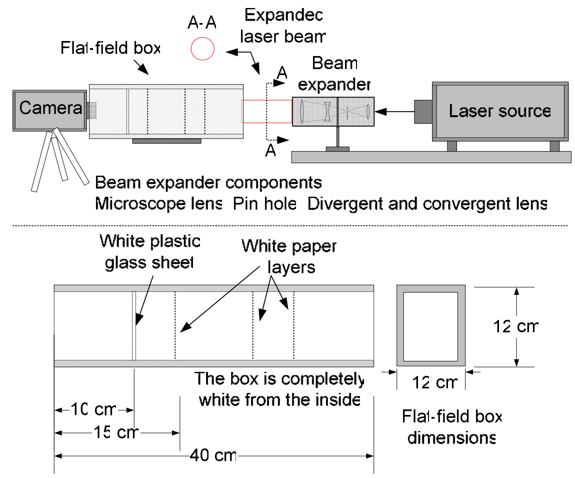

Fig.3: Flat-field image optical arrangement with the flat-field box dimensions

After all the necessary corrections were made, various weighting schemes could be used to improve the visual quality or to emphasize certain aspects of the images. Visualization of the data was performed on a PC using WinView (version V1.6.2.) in real time while running the experiments. ERGOvista (version 4.4.1) is another software package used during the data processing. This latter program is capable of generating two- and three-dimensional plots of the intensity data and extracting other information such as the statistical data used for computing the unmixedness which will be defined in a later section.

3.5 THE LSI SETUP

Two different optical arrangements were used for the LSI tests: (1) a lateral cross-section (see Fig.4) and (2) a vertical cross-section. In the first set-up, the lateral images produced by the light scattered from the alumina particles were recorded at 90º by the ICCD camera. The images were taken on the centerline plane of the test section assuming symmetry in the flows and geometry. To view the plane of interest in this case, the location of the camera and the optics table were illustrated in Fig.4. Only one plane was used when capturing the lateral images. For the second setup, the location of the camera and the optics table were moved from that of the first case, replacing each other. The camera was placed perpendicular to the face of the static mixer from the downstream location. For this set-up, the experimental analysis was performed at eight different axial distances from the exit plane of the static mixer, starting from the fuel cap exit plane, and planes located at 0, 5, 10, 15, 20, 25 and 30 cm respectively, see Fig.4 and Fig.5.

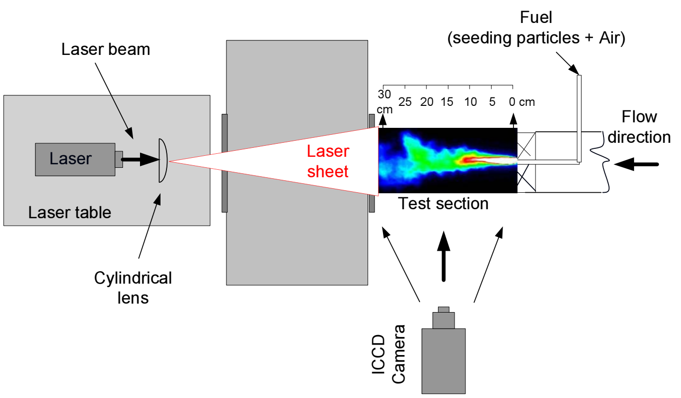

Fig.4: Schematic of the optical arrangement for lateral image setup

Optimizing the set-up and capturing the appropriate images using the LSI technique required a lot of trial and error. The first phase of the LSI experimental work program consisted of preliminary tests. These tests were performed for the two test configurations mentioned above to ensure consistent and reliable results. These preliminary tests helped to define the following parameters: test procedures, camera settings, laser intensity levels, the appropriate equipment locations, the location of the measurement planes (taking into consideration the effect of the premixer cylindrical shape and its wall thickness), image correction procedures, seeding conditions, and setting of the air and fuel flow rates. See Ref. [17] for more details.

3.6 THE EXPERIMENTAL VARIABLES

The key factors governing the turbulent mixing are velocity, density and momentum ratios (fuel-to-air), angle of fuel penetration, mixing path length, geometry of the fuel nozzles, the inlet velocity profiles of the fuel and the main stream [18]. In this study, the effects of some of the above mentioned parameters on the mixing process inside the duct burner premixer were investigated qualitatively using the LSI technique. During the LSI tests (main investigation [17]), the experimental variables were (1) premixer length (eight planes), (2) five flow mixers with single- and double-swirl mixer type designed with different angles, 15º and 30º, (3) five fuel injector caps having different injection angles and nozzle diameters, (4) equivalence ratio (ϕ = 0.5 (design condition) and ϕ = 0.3) and (5) the momentum ratio (0.23, 0.33, 0.39 and 0.64).

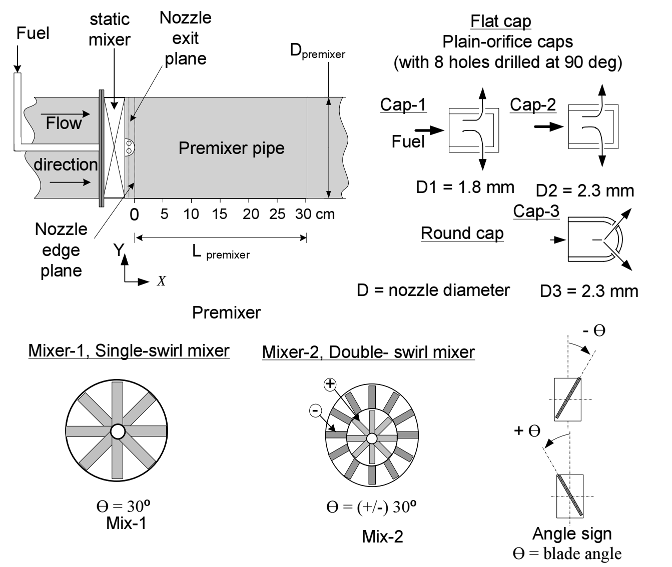

Fig.5: Schematic of the LSI geometrical variables

In this paper only the results of the following premixer components combination will be presented three different fuel caps (Cap-1, Cap-2 and Cap-3, see Fig.5). Each cap has 8 holes with 1.8 mm, 2.3 mm and 2.3 mm in diameter respectively. The fuel caps were tested with one single swirl mixer (Mix-1) and a double swirl static mixer (Mix-2). Fig.5 shows the schematic of the LSI geometrical variables studied in this paper with all the relevant dimensions and shapes. Table 1 presents the experimental matrix with a summary to the static mixers and the fuel caps characteristics used in this paper. The standard operating characteristics used in this investigation are summarized in Table 2.

Table 1: The experimental matrix

Run No.	Mixer type	Swirl No. (S)*	Swirler blade Ang. (º)	Fuel cap type	Fuel injection angle (º)	MMR Eq.1	ϕ
1	Mix-1	0.4	30	Cap-1	90	0.64	0.5
2	Mix-1	0.4	30	Cap-2	90	0.39	0.5
3	Mix-1	0.4	30	Cap-3	45	0.39	0.5
4	Mix-2	0.58	(+/-) 30	Cap-1	90	0.64	0.5
5	Mix-2	0.58	(+/-) 30	Cap-2	90	0.39	0.5
6	Mix-2	0.58	(+/-) 30	Cap-3	45	0.39	0.5

*Refer to Ramadan et al. (2009) for the way of calculating the swirl number (S)

Regarding the swirl mixers, it was mentioned that the main reason for this swirling flow is to improve the mixing between the eight fuel jets and the mainstream in a short distance. As the flame stability is not an issue in this design, the flow field inside the premixer pipe should be free from any low pressure zones (i.e., recirculation). The presence of low pressure zones in the premixer pipe during the combustion test could trigger flashback. Therefore all the static mixers used in this paper were designed with 30 degrees blade angle. This angle is selected to impart a low swirl level (S < 0.6) to the mainstream entering the premixer.

Table 2: Operating conditions used for the LSI tests

Parameter	Design value
Fuel flow rate	0.00475 kg/s
Fuel pipe inner diameter	10.21 mm
Methane molecular weight	0.01604 kg/mol
Fuel line pressure	2 psig
Fuel line Reynolds number (Re)	54,000
Fuel injectors Re (different nozzle diameters)	23,000 – 30,000
Duct burner (DB) total mass flow rate	0.7 kg/s
DB cone mass flow rate (25% of total mass flow rate)	0.186 kg/s
Mass ratio=MR_{LSI}=fuel flow rate/ cone mass flow rate	0.025
DB premixer pipe inner diameter	16.3 cm (6.407 in)
Premixer inlet velocity (upstream of the static mixer)	12 m/s
Oxidant (microturbine exhaust gases) temperature	200ºC
Premixer inlet Reynolds number	57,000
Turbulent intensity	≈ 10%
DB premixer components dimensions (e.g., mixers)	Ramadan et al. 2009
LSI model dimensions	See Fig.2
Uncertainty in velocity measurement	±3%

3.7 UNMIXEDNESS

One of the objectives of the LSI tests was to develop a measurement procedure to evaluate the mixing effectiveness for the different premixer geometries and operating conditions. Mixing can be defined as the process in which the inhomogeneous system is made homogeneous or uniform. Unmixedness is the term used in the literature as a measure of non-homogeneity [10, 13, 19, and 20]. Some researchers used the term coefficient of variation for this same unmixedness definition as a measure of uniformity. The spatial unmixedness, *Ux (*or unmixedness index), used in the present investigation, can be evaluated through quantitative analysis of light distribution (fuel concentration) on the LSI images and can be expressed as [13]:

$$Ux = \frac{\sigma_f}{m_f} \tag{3}$$

where σ_f is the standard deviation of the fuel concentration in a 2D plane and m_f is the mean of the fuel concentration over the same 2D plane.

Reference [13] used only the unmixedeness index to evaluate the mixing process. Ref. [20] used a normalized unmixedness to evaluate the mixing process. The unmixedness (the term coefficient of variation was used in their paper) was normalized by the unmixedness (coefficient of variation) at the nozzle exit where all the jet mass is injected. In the present investigation it was difficult to obtain the unmixedness from the images captured at the plane located at the fuel nozzle exit (the laser sheet passed over the fuel cap) as the fuel cap gave high light reflection. This reflection affects some of the images taken at the exit plane, therefore in the present investigation and for the purpose of ranking the different premixer geometries used, the unmixedness index was normalized by a quantity named Uo which is a function of the fuel to mainstream mass flow rate ratio (constant for all the tests).

The mixing effectiveness (η_{mix}) can then be defined as:

$$\eta_{mix} = \frac{Ux}{Uo} \tag{4}$$

where Uo is defined as:

$$Uo = \sqrt{\frac{1 - MR_{LSI}}{MR_{LSI}}} \tag{5}$$

where MR_{LSI} is the fuel jet-to- mainstream (air) mass flow ratio

$$MR_{LSI} = \frac{\dot{m}_{jet}}{\dot{m}_{flow}} \tag{6}$$

The η_{mix} has values between 0 and 1, where η_{mix} = 1 represents a maximum variance and thus corresponds to a totally unmixed mixture, a decreasing η_{mix} corresponds to increasing homogeneity of the premixed mixture, and $\eta_{mix} = 0$ represents the best mixing. The unmixedness parameter is referred to as the mixing effectiveness in this paper

4 RESULTS

Direct LSI images for the premixer flow field were captured to measure qualitatively the effect of different geometries on the mixing process. A number of flow configurations were investigated using two mixers and three fuel cap designs providing different flow conditions. The experimental analysis was performed for the two LSI test set-ups mentioned in the previous section. In the LSI tests the momentum ratio was maintained by keeping the main air stream (referred to in the paper as mainstream) flow rate constant and the fuel flow rate through the seeding system was controlled and varied. The velocity ratio was the characteristic parameter used to attain the momentum ratio. This then controls the penetration of the transverse injection into the mainstream air and the mixing of seeded air (fuel) and the mainstream air in the coaxial geometry [10]. A series of images were acquired including: the real data, the dark charge, the flat field and the background images. 10 to 20 images were obtained for each recording event. Each image contains 10 to 15 frames for averaging (a minimum of 100 frames at each location were averaged to improve the statistics and eliminate bias). The exposure time (refers to how long the camera is allowed to receive light) were varied between 20, 40, 60 and 80 ms. Most of the images used in the processing have the same exposure time (40 ms). The images were then processed to extract the necessary information needed for the evaluation of the different geometrical combinations studied. The selected approach was to evaluate the mixing process in the burner premixer using the LSI qualitative results (images) and to define an unmixedness index which could be evaluated through quantitative analysis of light distribution on the planar images. Under this mode of visualization (direct excitation mode), all the images of the mixing region show the spreading out of fuel (seeded flow) into the mainstream flow by the turbulent motion caused by the different static mixers. In this paper the particle concentration in an image is assumed proportional to the fuel concentration in the image [10].

For viewing and evaluating the growth of the fuel jets inside the premixer, scaling images were captured. The scaling images were used for sizing the premixer pipe and the fuel cap boundary in all the vertical cross-section images. The premixer cross-sectional boundary (premixer annulus region) is represented by the gray or red circles sketched on the images. The fuel cap was located approximately at the central ring (image centre).

The results presented in this section of the paper will cover some of the lateral and the vertical image set-up results at selected planes. Qualitative assessments and observations for some of these images will be discussed. The three-dimensional (3D) plot of the fuel concentration or fuel flow spread images for some planes will be shown for one run. The evaluation of the different geometrical combinations used by referring to the value of unmixedness will be presented. The last section will present the effect of the LSI study on the DB combustion process.

4.1 MIXING USING ROUND FUEL CAP (CAP-3)

As only one camera was used during the LSI phase, the lateral image shown in this section was taken under identical flow conditions as the vertical cross-sections cases, but at a different time. Therefore, due to the random nature of the fluid motion and other uncontrolled flow parameters (atmospheric pressure and temperature), the lateral images presented in this section may not coincide exactly with the vertical cross-sectional images presented for the same figure. The lateral images qualitatively gave an insight into what the flow or the fuel spread looks like in the lateral sections.

Figure 6 shows the effect of using the single swirl mixer, Mix-1, and the round fuel cap design (Cap-3 with 45º injection angle) on the fuel-air mixing. Vertical and lateral cross-sectional images are presented in this figure. The figure shows that at the 5 cm plane the fuel jets are not completely combined or mixed with each other. High fuel concentration spots distributed around the fuel cap are clearly visible. As the distance increases downstream, the fuel jets mix together and occupy more of the premixer area. The figure clearly shows the rotation of the flow field. The image at the end of the premixer (30 cm) shows an inhomogeneous spread of the fuel in the premixer cross-section. The mixing is shown to slowly improved from the first station (5 cm) to the premixer end plane.

Figure 7 presents the results for the counter swirl flow mixer, Mix-2, which shows the wider fuel spread across the lateral cross-section. The lateral image shows that this mixer bends the fuel jets towards the premixer centre, causing the fuel jet to mix with mainstream air rapidly. The images in Fig. 7 show that this mixer produces better mixing than Mix-1. The fuel spread grows to a doughnut shape at the premixer mid plane (15 cm). The images indicate that the area occupied by the injected fuel at 10, 15 and 30 cm planes is greater with the use of the double mixer than in the first case where the single swirl mixer, Mix-1, is used.

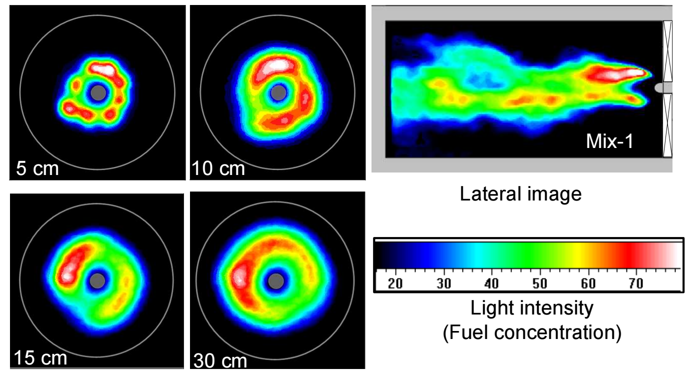

Fig.6: Vertical and lateral cross-sectional LSI images (Mix-1 and Cap-3 with ϕ = 0.5).

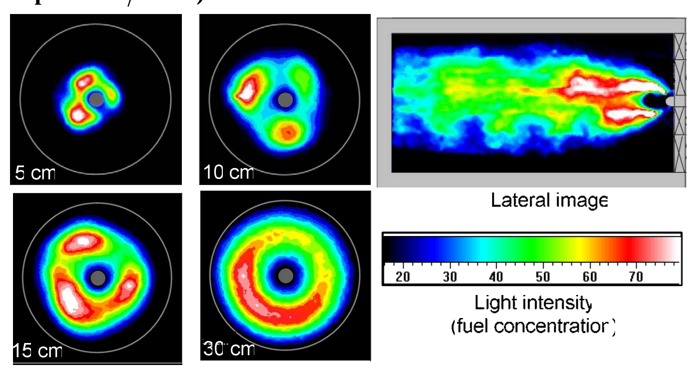

Fig.7: Vertical and lateral cross-sectional LSI images ((Mix-2 and Cap-3 with ϕ = 0.5)

Figure 8 shows the 3D plots for the images taken at all the four planes of measurements presented in Fig.7. These plots clearly show how the image intensity peaks grow, rotate and combine in proportion to the fuel concentration as the distance increases downstream of the fuel cap. Comparing the vertical cross-sectional images with the 3D plots gives a clear qualitative idea about how fuel spreads in the swirling main flow.

4.2 MIXING USING FLAT CAPS (CAP-1& 2)

Figure 9 is a direct comparison of using mixers, Mix-1 and Mix-2, with Cap-2 (90º injection angle). These tests were performed at the same operating conditions as that presented in the previous results, Figs. 7 and 8 (ϕ = 0.5, MMR = 0.39). Fig. 9 shows the change in fuel concentration or the fuel spread inside the swirling cross-flow at 3 different locations for both mixers. The images show that as the distance increases downstream, the spread of the fuel is increased and becomes more homogeneous. By close observation of the last two images in Fig.9 (at the 15 cm and 30 cm planes) one can observe some similarity. It could be said that the fuel jet spreads slowly in this region. However, compared to the 45º fuel injection, Cap-3 (e.g., Fig.6 and Fig.7), the fuel spread (homogeneity) is greater with the radial fuel injection, Cap-2. At 5 cm, the spread of the fuel occupies approximately 22 percent of the premixer cross-sectional area in Fig.6 or Fig.7 while at the same distance in Fig.9, the fuel jet covers more than 85 percent of the premixer cross-sectional area.

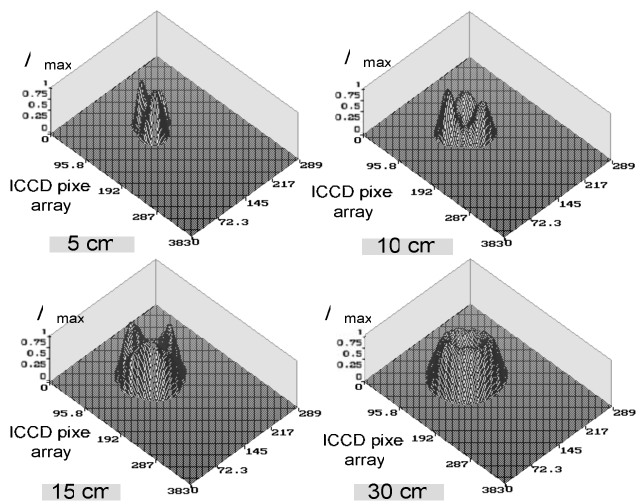

Fig.8: 3D plots for the vertical cross-sectional LSI images for Mix-2, Cap-3 and ϕ=0.5 (I is the light intensity normalized by I $_{max}$.)

4.2.1 Jet penetration in swirling flow. In this subsection the radial fuel jet penetration in the swirling mainstream will be briefly discussed. The fuel jet penetration is defined as the measure of the maximum radial distance the fuel penetrates into the body of the co-flow at a given downstream distance [21]. Fig.10 shows the effect of using different mixers with Cap-1 (MMR of 0.64) on the radial fuel jet penetration. The figure clearly shows the eight fuel jets (fingers) penetrating through the swirling cross flow. These vertical cross-sectional images were taken at the fuel nozzle exit plane. The penetration ratio (PR) is shown on the image for each mixer. Ref. [21] defined the penetration ratio as the ratio of the penetration distance to the combustor liner diameter. In the present work, the premixer pipe diameter was used in place of the combustor liner diameter. The optimum PR value for a gas turbine combustor is 0.33 [21]. The flow conditions presented in Fig. 10 show a good value of PR. Another result observed from Fig. 10 is the quick distortion of the normal circular jet cross-section at the top of each jet finger to an oval deformed shape. This fact will be clearly shown in later images where the vertical cross-sectional images are taken at the edge of the fuel cap plane for the different mixers at a location of 1 cm downstream of the nozzle exit.

Figure 10 also shows the direction of rotation of the swirling flow. The single-swirl mixer rotates the flow according to the blade angle direction, therefore Mix-1 introduces anticlockwise rotation to the flow stream resulting from its negative (-ve) blade angle, see Fig.5 for the angle sign. For the double-swirl mixer, Mix-2 shows a clockwise rotation due to its inner swirl blade angle (+ve). Later colored images will show the direction of rotation clearly.

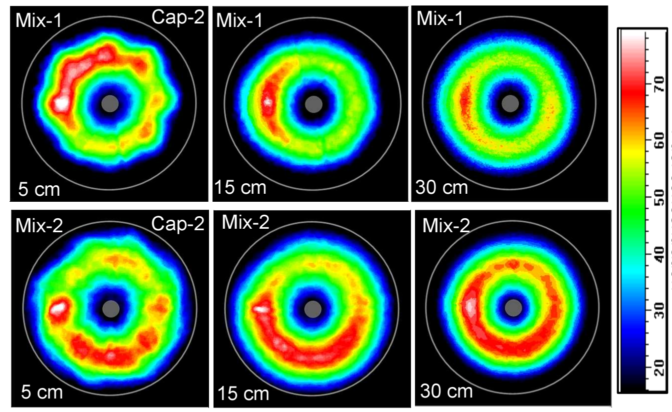

Fig.9: Vertical cross-sectional LSI images (Mix-1 and Cap-2 with ϕ = 0.5)

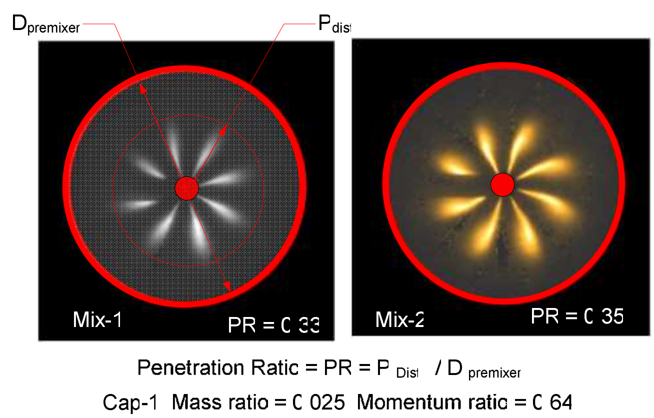

Fig.10: Effect of different mixers on penetration ratio (vertical cross-sections for Cap-1)

Figure 11 shows the change in the fuel spread inside the swirling cross-flow at the first two locations for mixers Mix-1 and Mix-2 when tested with Cap-1 (90º angle and MMR=0.64). The left image taken at the nozzle exit was used here in this figure, just to show the original rotation of the imported swirling flow. The other image was captured at the edge of the fuel cap, which is 1 cm downstream from the nozzle exit plane (0.0 cm). By close examination of the LSI images at the fuel cap edge and the nozzle exit plane images one can observe the direction of rotation of the two images and how the fuel jets were distorted and transformed into swirling jets. The tangential movement of these jets is in the opposite direction to the initial movement observed in the nozzle exit plane image (the direction of rotation is shown in the images). Similar observations were reported by Ref. [22]. At the fuel cap edge plane, the image shows the distinct structure of the distorted inlet fuel jets (small swirls) in a ring, with local maximum fuel concentration at roughly the same radius from the premixer centre axis. Also, one can observe that the small swirls are connected to a central disc. The view of the central disc is not completely shown due to the fuel cap mask used to avoid the reflected light.

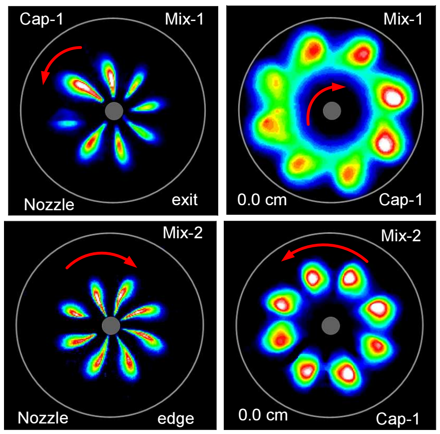

Fig.11: Transformation of the fuel jets to swirling jets

Both results presented in Figures 10 and 11 qualitatively give an idea of how far the radial fuel jet trajectories penetrate through a swirling cross-flow and how it is affected by the different swirl and fuel cap designs. The swirling cross-flow also forces the fuel jets to bend due to the existence of pressure differences across the jet. Mix-2 shows the stronger effect compared with Mix-1. It bends the jet over in the direction of the swirling cross flow.

4.3 UNMIXEDNESS RESULTS

In this section the results of the mixing effectiveness are presented at several cross-sections downstream of the static mixer for the different geometric combinations studied. Only selected cases were analyzed by comparing these computed results. The computed results (Ux/Uo) are plotted versus axial distance for all cases studied. For a better presentation the axial distance was normalized by the premixer diameter.

Figure 12 shows the variation of mixing effectiveness with the axial distance along the premixer for different fuel cap designs tested with Mix-1. At the fuel cap nozzle where all the jet fuel mass is injected, (Ux/Uo) reaches its maximum value and then decreases downstream as the jet spreads and mixes with the swirling cross-flow. It is clearly noticeable that Cap-3 has the highest unmixedness values at all the axial locations measured. This is the result of the fuel injection angle (45º), compared to the radial injection caps (Cap-1 and Cap-2). This result can also be concluded by direct observation of the LSI images discussed in the previous sections. Fig.12 also shows that for Cap-3 the mixing effectiveness improves (decreases) slowly as the axial distance increases and still does not attain the best mixing effectiveness at the end of premixer. On the contrary, for the other flat caps (radial fuel injection) the mixing effectiveness reaches its maximum (lower value) even before the premixer mid plane ($X/D_{premixer}$ = 1). From the two flat caps Cap-2 indicates the lowest unmixedness values at all the planes.

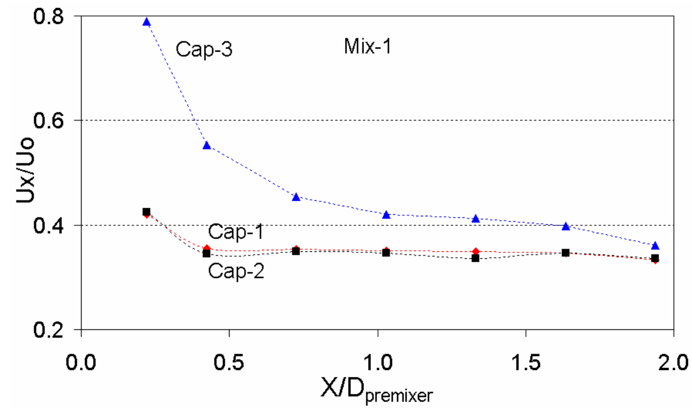

Fig.12: Effect of fuel injection angle on mixing effectiveness

Figure 13 shows the effect of fuel injection angle on mixing effectiveness for the double-swirl mixer, Mix-2. Similar results as that concluded from Fig.12 are observed in Fig.13. Cap-3 has the highest unmixedness values and Cap-2 has the lowest at all the measured planes.

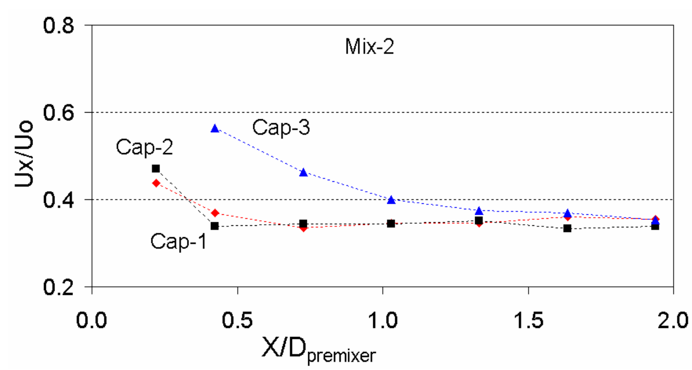

Fig.13: Effect of fuel injection angle on mixing effectiveness

According to the results discussed in subsections 4.1, 4.2, and 4.3, the combination of Mix-2 with Cap-2, shows the best premixer and produces the best fuel-air mixing results. This combination was selected and manufactured for the second stage of testing the combustion tests. The following section covers some of the combustion results.

4.4 COMBUSTION RESULTS

To support the results obtained from the LSI tests, it was decided to perform the combustion tests with premixer parameters that provide completely different mixing behaviors (good and poor mixing). Fuel injection angle is the parameter selected for this discussion. Cap-2 (90º) and Cap-3 (45º) have similar designs (number and diameter of fuel injecting holes), but with different injection angles. From the observation of the LSI results, Cap-3 shows poor mixing results compared to Cap-2. The mixing comparisons between the two caps when the LSI technique was used were presented in Fig. 13. In this subsection, the effect of fuel injection angle and the static mixer design on the performance of the duct burner and the mixing process inside the premixer will be presented and discussed.

Figures 14 (a) and (b) show the effect of fuel injection angles as a function of firing rate (FR) on the DB performance.

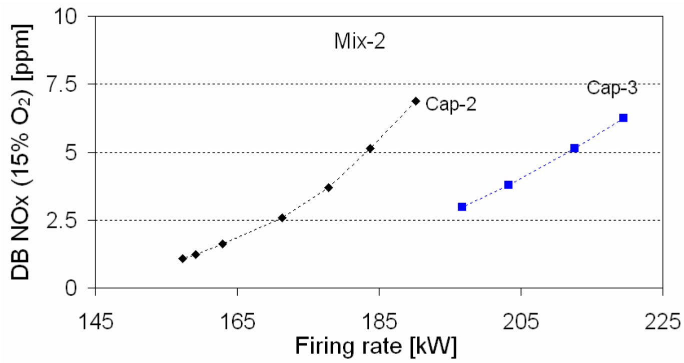

(a) DB NOx emissions

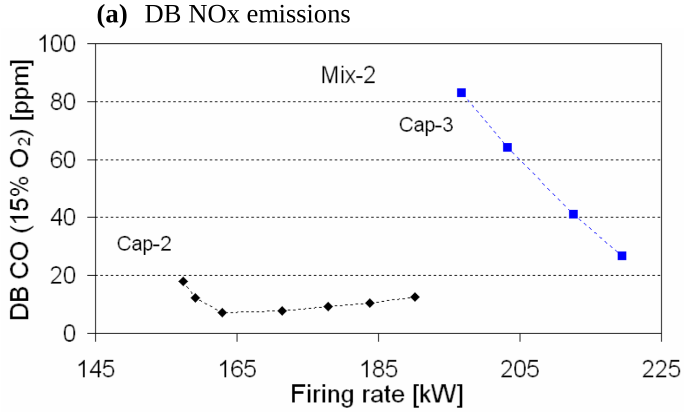

(b) DB CO emissions

Fig.14: Effect of firing rate and fuel injection angle on duct burner performance (Mix-2)

The DB configurations that were tested were Mix-2 (which provides the best LSI results) with Cap-2 and Cap-3. NOx emissions are shown in Fig.14 (a) and Fig.14 (b) shows the CO emissions. Cap-2 showed a stable operating range from 157 to 190 kW with NOx emissions ranging from 1 to 7 ppm. CO emissions ranged from 7.2 to 18 ppm. During the combustion tests of Cap-3, the fuel flow rate supplied to the duct burner was not sufficient to allow tests to be carried out at the same fuel flow rate as that used with Cap-2. The flame obtained during these trials was not stable and quickly blew off. The reason for that was the poor mixing provided by Cap-3 as the temperature profiles below will show. Good mixing improves the ability of the fuel to burn. The fuel flow rate was increased to achieve a flammable mixture and stable conditions. The attempts were successful and continuous combustion over the mesh surface was achieved but at high firing rates for the Cap-3 tests. Stretched blue flames were observed and high CO emissions were recorded. The high CO emissions values were due to the incomplete combustion caused by poor mixing. Local flame instability was observed on the lower part of the conical burner especially at lower firing rates with Cap-3. From Figures 14 (a) and (b), NOx emissions with Cap-3 were from 3 to 6 ppm and CO emissions were from 27 to 96 ppm.

To further understand effect of the mixing process inside the premixer, temperature measurements were conducted by traversing a K-type thermocouple across the premixer exit plane. The uniformity of these temperature profiles indicates good mixing behaviour between the oxidant and the fuel supplied to the burner. Fig.15 shows the effect of the fuel injection angle on the temperature profile for the same case presented in Figures 14 (a) and (b). Cap-2 shows very good temperature profile uniformity (fairly constant over all the premixer cross-section) compared to the results with Cap-3. This result again proves the effectiveness of the LSI technique used in this investigation for identifying mixing uniformity.

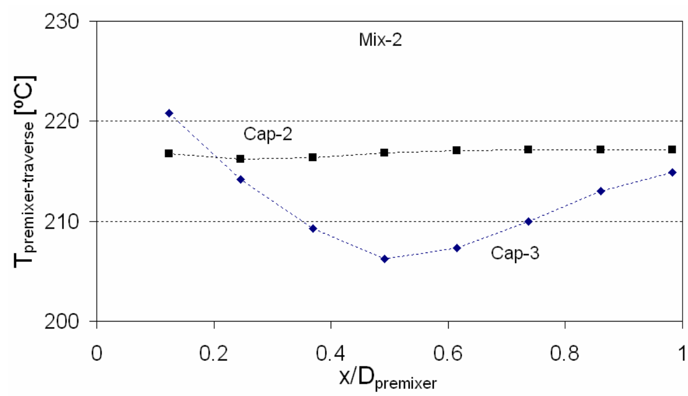

Fig.15: Effect of fuel injection angle on mixture (oxidant/fuel) temperature profiles at the premixer exit plane, Mix-2

Figure 16 shows the effect of firing rate and mixer design on DB performance for the burner configuration tested (Cap-2 was used in this combination). The figure labelled (a) presents NOx emissions and (b) CO emissions. The double-swirl mixer, Mix-2, which has a higher swirl strength, shows lower NOx and CO emissions. This is attributed to better mixing provided by the double-swirl mixer. For the single-swirl mixer, the stable operating range shifts and extends towards the lower firing rate values. The decrease of the stable operating range for the double-swirl mixer was due to the increase in the swirl strength.

5 CONCLUSIONS

The mixing process in the premixer of the conical wire-mesh DB was studied qualitatively using the laser sheet illumination (LSI) technique. A quasi-quantitative technique was used to rank the relative mixing performance of the different types of mixers and fuel cap tested. The LSI images provided a qualitative picture of the flow conditions analyzed in this work. The direct observation of the vertical and lateral cross-sectional LSI images along with the 3D plots assisted in ranking the different geometrical combinations used.

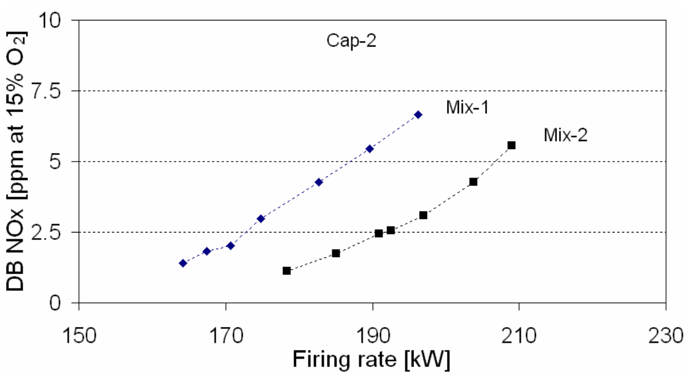

(a) DB NOx emissions

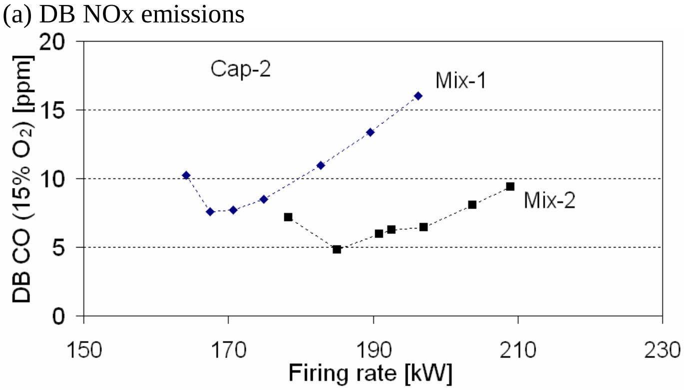

(b) DB CO emissions

Fig.16: Effect of firing rate and mixers design on DB performance

The LSI results obtained were helpful to gain a better comprehension of the mixing process in the burner premixer, providing useful information for the optimization of burner design and operating conditions. The resulting burner designs were studied in combustion tests to arrive at a final design that is expected to achieve high combustion efficiency and reduced NOx and CO emissions. The selected premixer components that were used in the combustion test and their encouraging results regarding the single digit emissions, proves the effectiveness of the LSI technique used in this investigation.

During the combustion tests the DB displayed a stable low emission operation throughout the surface firing rate range of 148–328 kW (only the emission data for firing rates less than 215 kW are presented in this paper). The DB successfully raised the micro-turbine exhaust gases temperature from about 227ºC to as high as 700ºC with NOx and CO emissions of less than 10 ppmv (corrected to 15 percent O_2). Refer to Ref. [1] and Ref. [17] for more details on the combustion results.

ACKNOWLEDGMENTS

This study was supported by CanmetENERGY Centre, Ottawa, ON, Canada.

REFERENCES

[1] Ramadan, O. B., Gauthier, J. E. D., Hughes, P. M., and Brandon, R., 2007, “Experimental Investigation and Evaluation of a Low NOx Natural Gas-Fired Mesh Duct Burner,” ASME Paper No. GT2007-28350.

[2] Ramadan O. B., Gauthier J. E. D., Hughes P. M., Brandon R., 2009, “Design Procedure of Novel Micro-Turbine Low NOx Conical Wire-Mesh Duct Burner”, Transactions of the ASME, Journal of Engineering for Gas Turbine and Power, Vol.131, no.6, pp.062301-8

[3] Tavoularis, S., 2005, “Measurement in Fluid Mechanics”, First Edition, Cambridge University Press.

[4] Goldstein, R. J., 1996, “Fluid Mechanics Measurements.” Second Edition, Taylor and Francis.

[5] Lauterborn, W. and Vogel, A, 1984, “Modern Optical Techniques in Fluid Mechanics.” Annu Rev of Fluid Mech. 16, pp. 223-244.

[6] Merzkirch, W., 1987, “Flow Visualization”, Academic Press, New York.

[7] Eckbreth, A. C., 1988, “Laser Diagnostics for Combustion Temperature and Species” , Abacus Press.

[8] Zhao H., and Ladommatos N., 1998, “Optical diagnostics for in-cylinder mixture formation measurements in IC engines”, Progr Energy Combust Sci 24, pp. 297–336.

[9] Gal, P. Le, Farrugi, N., Greenhalgh, D.A., 1999, “Laser Sheet Drop Sizing of Dense Sprays.” Optics and Laser Technology, Vol. 31, pp.75-83.

[10] Solero, G., and Coghe, A., 2000, “Effect of Injection Typology on Turbulent Homogeneous Mixing in a Natural Gas Swirl Burner”, Experimental Thermal and Fluid Science, Vol. 21, Issues 1-3, Pages 162-170.

[11] Harinaldi, T. U. and Mizomoto, M., 2001, “Laser Sheet Imaging of Recirculation Zone of Backward-Facing Step Flow with Gas Injection.” Journal of Chemical Engineering of Japan, Vol. 34, No. 3, pp. 351-359.

[12] Stowe, R. A., 2001, “Performance Prediction of a Ducted Rocket Combustor.” Ph.D. Thesis, Laval University, Quebec, Canada.

[13] Yimer, I., and Campbell, I., 2002. “Parametric Study to Optimize Air/Fuel Mixing for Lean, Premix Combustion system.” Proceedings of the International Joint Power Generation Conference. ASME, Phoenix, Arizona, USA, (IJPGC2002-26086).

[14] Adam A., Leick P., Bittlinger G. Schulz C., 2009, “Visualization of the evaporation of a diesel spray using combined Mie and Rayleigh scattering techniques”, Exp. Fluids 47, pp. 439–449

[15] Thiery, L., J. Prenel, R. Porcar, 1996, “Theoretical and experimental intensity analysis of Laser Light Sheets for Flow Visualization.” Optics Communications, Vol. 123, pp 801-809.

[16] Watkins, C., Sadun, A., Marenka, S., 1993, “Modern Image Processing: Warping, Morphing, and Classical Techniques”, Academic Press Professional, UK.

[17] Ramadan O. B., [2008], “Design and Evaluation of a Low NOx Natural Gas-Fired Conical Wire-Mesh Duct Burner for a Micro-Cogeneration Unit”, PhD. Thesis, Carleton University, Ottawa, ON, Canada.

[18] Turns, S. R. 2000. “An Introduction to combustion: Concepts and Applications”,Second Edition, New York, McGraw- Hill.

[19] Turek, L. J., Chaos, M., Dawson, R. W., Chen, R. H., 2005, “An Investigation of the Effect of Swirl Vane Angle on Fuel Concentration and Velocity Fields Gas Turbine Mixers”, GT2005-68152, ASME Turbo Expo: Power for Land, Sea and Air, Reno-Tahoe, Nevada, USA.

[20] Bakker, A., LaRoche, R. D., and Marshall, E. M., 2000, “Laminar Flow in Static Mixers with Helical Elements.” The online CFM Book, http://www. Bakker.org/cfm.

[21] Sawyer, J. W., 1985, “Sawyer’s Gas Turbine Engineering Handbook”, 3rd ed., Turbomachinery International, Nor-walk, CT.

[22] Barrue, H., Karoui, A., Sauze, N. Le., Costes, J, Illy, F., 2001, “Comparison of Aerodynamics and Mixing Mechanisms of Three Mixers: Oxynator Gas-Gas Mixer, KMA and SMI Static Mixers”, Chemical Engineering Journal, 84, pp.343-354, Elsevier.